

# We are IntechOpen, the world's leading publisher of Open Access books Built by scientists, for scientists

6,900

Open access books available

186,000

International authors and editors

200M

Downloads

Our authors are among the

154

Countries delivered to

TOP 1%

most cited scientists

12.2%

Contributors from top 500 universities



WEB OF SCIENCE™

Selection of our books indexed in the Book Citation Index  
in Web of Science™ Core Collection (BKCI)

Interested in publishing with us?  
Contact [book.department@intechopen.com](mailto:book.department@intechopen.com)

Numbers displayed above are based on latest data collected.  
For more information visit [www.intechopen.com](http://www.intechopen.com)



---

# Two-Step Sintering of Ceramics

---

Ubenthiran Sutharsini,  
Murugathas Thanihachelvan and Ramesh Singh

Additional information is available at the end of the chapter

<http://dx.doi.org/10.5772/68083>

---

## Abstract

Sintering is a critical phase in the production of ceramic bodies. By controlling the density and microstructure formation, sintering now emerged as a processing technology of ceramic materials. Tailoring the structural, mechanical, electrical, magnetic and optical properties is widening the application of ceramics in various fields. Recently, many advanced sintering methods have reported to fabricate ceramic materials with controlled properties. Two-stage sintering (TSS) is one of the simple and cost-effective methods to obtain near-theoretical density materials with controlled grain growth without adding any dopants. Many recent works have reported the use of TSS as a processing method to fabricate nanoceramics for various applications. With this background, this chapter reviews the advantages of TSS in ceramic preparation based on properties and materials and explores the future directions.

**Keywords:** two-step sintering, grain growth, ceramic properties, densification, sintering mechanism

---

## 1. Introduction

Highly dense ceramics with smaller grain size are widely used in high-performance applications in extreme conditions. Sintering is the responsible step for densification of ceramic bodies, and due to its influence on the properties of the material, sintering is also emerging as a new fabrication method. Controlling the powder size [1], use of sintering additives [2], green body density [3–5] and sintering environment [6, 7] and using new sintering methods such as microwave sintering [8, 9], pressure-assisted sintering [10], spark plasma sintering [11] and field-assisted sintering [3] are used for fabrication of dense and fine-grained ceramics. But these may destroy the unique properties of ceramics [12]. Also the applications of new

sintering techniques are limited by low mass productivity, and they are not economically feasible. Two-stage sintering (TSS) is an effective way to achieve fine-grained microstructured ceramics with high densification and relatively low cost. TSS method is successfully applied for all types of ceramics such as structural ceramics, bioceramics, ferrites, piezoelectric ceramics and electrolyte ceramics. Most of the ceramics exhibit controlled or no grain growth in the final stage of sintering and achieved near-theoretical densities. The fine-grained microstructure enhances the mechanical, electrical, magnetic as well as piezoelectric properties of ceramics which widen the applications of ceramics.

TSS consists of heating the samples in two stages. Different sintering profiles were applied in TSS. Generalized diagrams of TSS are shown in **Figure 1(a)** and **(b)**. In the sintering profile 1, the first-step sintering temperature is higher than the second-step sintering temperature, and the first-step holding time is lower than the second-step holding time. Sintering profile 2 is the other way around. The first-step sintering temperature is lower than the second-step sintering temperature, and the first-step holding time is normally higher than the second-step holding time.

In addition, a modified two-step sintering profile is also reported with a cooling step (to room temperature) in between first and second step sintering [2, 13, 14]. Especially, this method used different sintering methods at first and second steps [2, 14].

This chapter mainly focuses on TSS with high first-step sintering temperature. The mechanism of densification with controlled grain growth is explained briefly, and the extended applications of TSS on different ceramics are outlined. Finally the chapter concludes the current trends and challenges of TSS as a fabrication method.

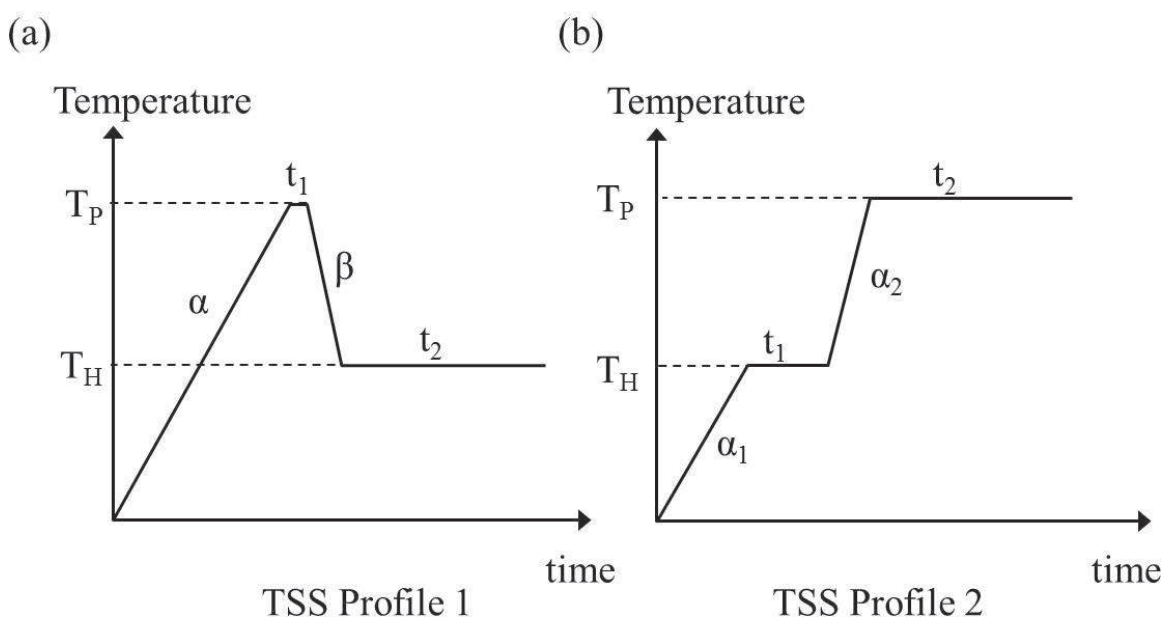


**Figure 1.** Different sintering profiles used in TSS (a) with high first-step sintering temperature and (b) with a low first-step sintering temperature.

## 2. TSS with high first-step sintering temperature

TSS with a high first-step sintering temperature is widely used to obtain fully dense ceramics with controlled grain growth due to lower second-step sintering temperature. The sintering profile for TSS with higher first-step sintering temperature is depicted in **Figure 1(a)**. Sintering profile 1 also has few categories based on other sintering parameters:

- Holding time ( $t_1$ ): The first-step sintering holding time ( $t_1$ ) is assumed to be zero in few studies, and others hold for a few minutes at temperature  $T_p$ .
- Cooling rate ( $\beta$ ): Few studies assumed sample rapidly cooled from first sintering temperature ( $T_p$ ) to second-step sintering temperature ( $T_H$ ), and others used controlled cooling rates.

The successful TSS method using profile 1 was first introduced for  $Y_2O_3$  by Chen and Wang [15]. In the TSS method, the ceramic samples were heated to a higher temperature to achieve critical density and then immediately cooled to lower temperature and held at that temperature for long holding time to achieve full densification. Density of the sintered sample increased with increasing grain size during the first-step sintering. However, grain growth is controlled at the second stage of sintering, and grain size versus density graph is horizontal at the final stage of the sintering [15]. Similar relationship was observed for other ceramics such as Mg, Nb-doped  $Y_2O_3$  [15], ZnO [16], Ni-Cu-Zn ferrite ceramics,  $BaTiO_3$  [17] and  $0.89Bi_{0.5}Na_{0.5}TiO_3 \cdot 0.06BaTiO_3 \cdot 0.05K_{0.5}Na_{0.5}NbO_3$  lead free antiferroelectric ceramics [18]. However, the most crucial task in this method is to identify suitable sintering parameters such as heating and cooling rate, the first- and second-step sintering temperatures, holding times and sintering atmospheres.

### 2.1. Sintering mechanism

TSS with a high first-step sintering temperature is widely used to obtain fully dense ceramics with controlled grain growth due to lower second-step sintering temperature. The mechanism for controlled grain growth in TSS with higher first-step sintering temperature was firstly proposed by Chen and Wang [15], for a TSS study on  $Y_2O_3$  ceramics, and it is widely accepted and verified for other ceramics.

The general mechanisms that are responsible for densification during sintering are grain boundary migration and grain boundary diffusion. Grain boundary migration is responsible for the rapid grain growth in the final stage of conventional sintering. The densification of ceramics with grain growth suppression at the second-step sintering can be explained by the absence of grain boundary migration during the second-step sintering as described in **Figure 2**. In conventional single-step sintering (SSS), the grain growth is accelerated due to grain boundary migration and grain boundary diffusion in the final stage of sintering. Rapid cooling before the second stage of sintering freezes the microstructure by immobilizing the triple-point junctions and continues densification will be achieved by grain boundary diffusion.

For a successful TSS profile with higher first-step sintering temperature, few conditions should be achieved at the end of first-step sintering. The sample must be reaching a critical density at

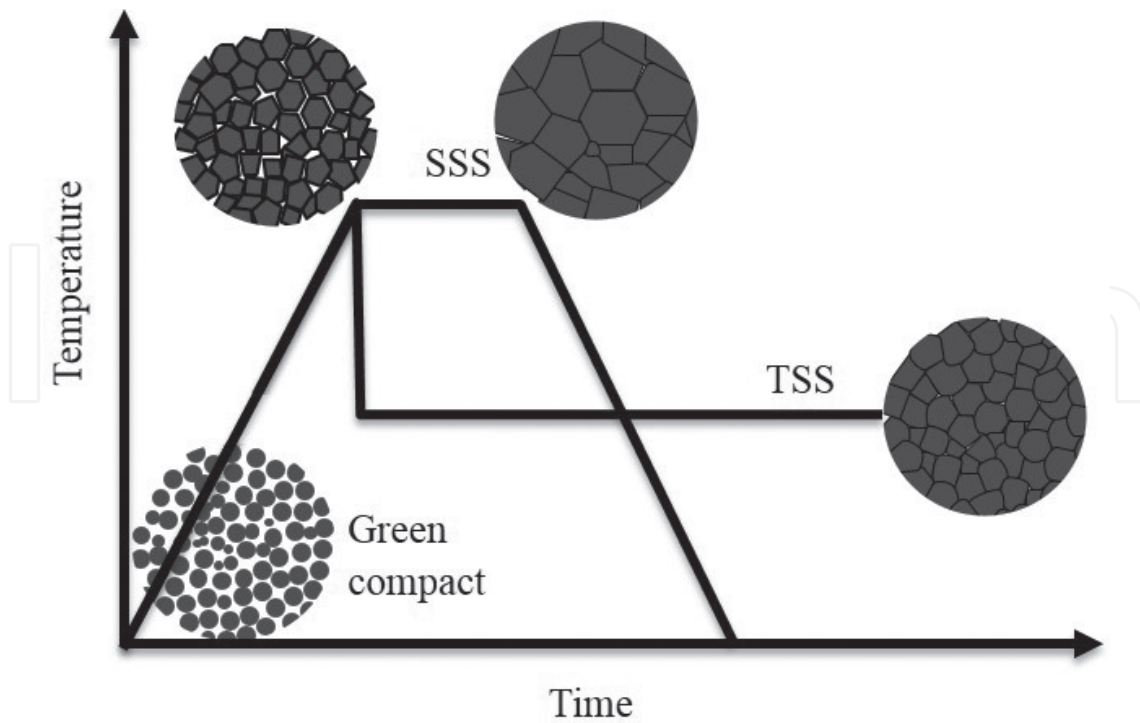


**Figure 2.** Schematic of densification of ceramics with grain growth during conventional single-step sintering (SSS) and densification without grain growth at lower second-step temperature during TSS with higher first-step temperature.

the end of the first-step sintering so that the densification is active in the final sintering step. This critical density depends on the material. As reported, the critical density to be achieved at the end of the first-step sintering for  $Y_2O_3$  is 75% [15],  $BaTiO_3$  is 73% [17] and Ni-Cu-Zn ferrite ceramic is 76% [17]. The critical density is essential to ensure that the pores in the material are subcritical and unstable against shrinkage which can be filled by grain boundary diffusion in the second-step sintering.

A kinetic window will be used to identify the optimum range of the first-step sintering temperature for successful TSS. **Figure 3** illustrates the kinetic window for pure and Mg- and Nb-doped  $Y_2O_3$ . The filled squares between the lower and upper limits of the first-step sintering represent the successful second-step sintering. The open squares above the upper limit of the first-step sintering show grain growth during the second step and below the lower limit represents the failed attempts to achieve full densification. It can also be concluded that the kinetic window can be shifted up and down along the first-step temperature axis with the addition of dopants. So far, the kinetic windows have been proposed to  $Y_2O_3$  [15, 19], Mg, Nb-doped  $Y_2O_3$  [15, 19], ZnO [20], Ni-Cu-Zn ferrite [17],  $BaTiO_3$  [17] and  $(1-x) BiScO_{3-x} PbTiO_3$  (BSPT) [21].

Another important study on exploring the mechanism of grain growth suppression in TSS with higher first-step sintering temperature was reported on ZnO ceramics. The transmission electron microscope (TEM) images of a TSS sample at a first-step sintering temperature of 800°C for 60 s and a second-step sintering temperature of 750°C for 20 h (**Figure 4(a)**) and a conventionally sintered ZnO at 1100°C (**Figure 4(b)**) were examined for the evidences of grain boundary migration. Ten different grain boundary zones were analysed from the TEM

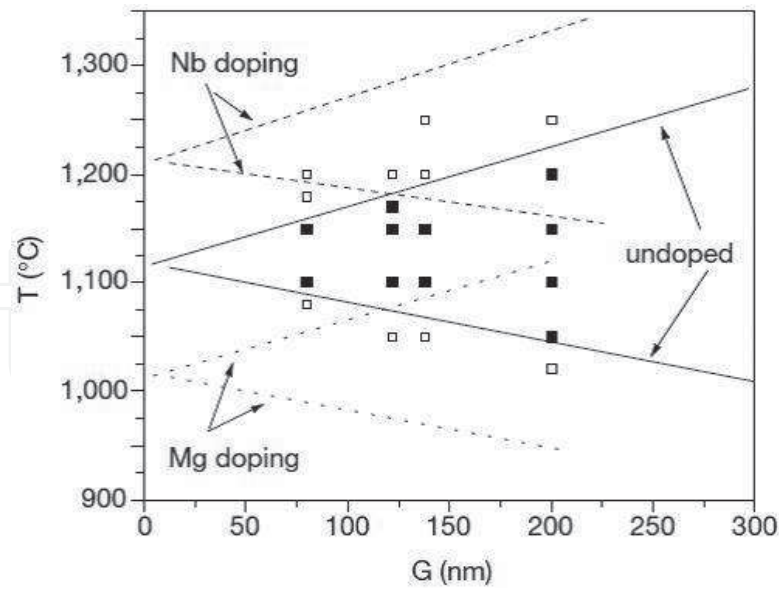


**Figure 3.** Kinetic window for pure, Mg- and Nb-doped  $Y_2O_3$  ( $T$  is the first-step sintering temperature and  $G$  is grain size) [15].

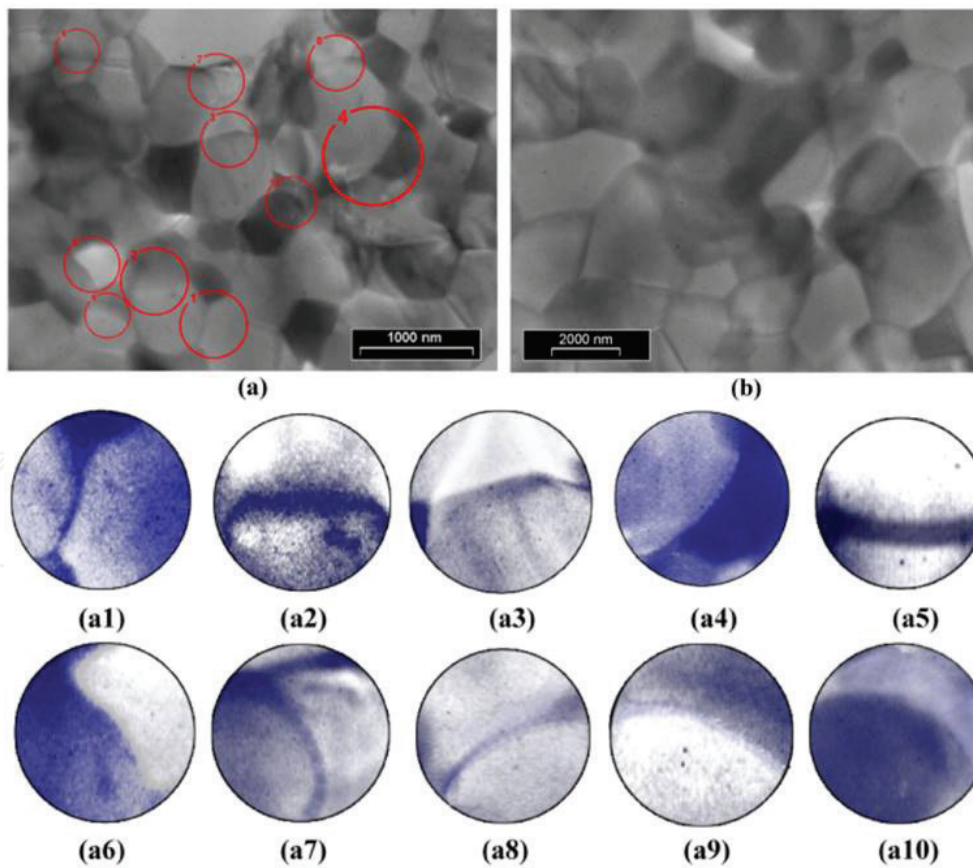


**Figure 4.** TEM images of the ZnO samples sintered (a) using TSS profile with the first-step sintering temperature of  $800^\circ\text{C}$  for 60 s and a second-step sintering temperature of  $750^\circ\text{C}$  for 72,000 s, (b) conventionally at  $1100^\circ\text{C}$  and (a1)–(a10) magnified images of grain boundaries marked in circles at (a) [22].

image of TSSZnO sample. As can be seen in **Figure 4(a1–a10)**, junctions seem to have pinned the boundaries of growing grains, and the curvature of these boundaries resulted from the mentioned immobilized triple points. However, no similar zones are observed in the TEM images from conventionally sintered samples (**Figure 4(b)**).

## 2.2. Effect of TSS with high first-step temperature on properties of ceramics

By successfully controlling the grain growth, the TSS with higher first-step sintering temperature is used to fabricate many ceramic materials with enhanced properties that are used for advanced applications [23]. So far TSS is applied for 3 mol% yttria-stabilized tetragonal zirconia polycrystals (3Y-TZP) [1, 4, 5, 8, 24–31], 8 mol% yttria-stabilized zirconia (8YSZ) [3, 5, 9, 24, 32–34],  $\text{Al}_2\text{O}_3$  [5, 24, 25, 35–43], doped alumina [37, 41], yttrium aluminium garnet (YAG) [44, 45], magnesium aluminium silicate [46], corundum [42, 43], hydroxyapatite [14, 47–50], forsterite ( $\text{Mg}_2\text{SiO}_4$ ) [51],  $\text{TiO}_2$  [11, 52–54],  $\text{SrTiO}_3$  [25] ( $\text{K}_x\text{Na}_{1-x}$ )  $\text{NbO}_3$  (KNN) ceramic [12, 55–57], SiC [58–60] and  $\text{Si}_3\text{N}_4$  [2] and used for several applications. This section outlined the changes in properties of various ceramics sintered using different TSS profiles.

### 2.2.1. Sintering of zirconia ceramics

Pure zirconia has three crystallographic structures, monoclinic, tetragonal and cubic. At room temperature monoclinic is stable. In pure form, zirconia has very low appeal for use as engineering ceramic due to reverse transformation on cooling resulting in severe cracking associated with volume expansion ( $\sim 3\%$ ) to the monoclinic phase. In order to overcome this problem, stabilizers such as MgO, CaO and  $\text{Y}_2\text{O}_3$  are added. Stabilizers reduce the change of chemical free energy and stabilize tetragonal or cubic phase at room temperature.

#### 2.2.1.1. 3Y-TZP ceramics

3Y-TZP is also known as ceramic steel, which exhibits excellent mechanical properties. It is found in many applications, such as cutting tools, grinding media for powders, extrusion dies and biomedical application. Fully dense ceramics with uniform microstructure and fine grain size is essential to stabilize the tetragonal phase as well as to improve the mechanical properties such as hardness and toughness. There are many TSS profiles conducted to control the grain growth of Y-TZP ceramics [1, 4, 5, 8, 24–31, 61]. Only few researchers successfully obtained fully dense ceramics with controlled grain growth ( $< 5$  times of powder size) [1, 4, 5, 25, 28, 29, 31, 62]. Among these studies, Binner et al. [31] and others [1, 29] successfully sintered nanostructured zirconia ceramics. Binner et al. [31] achieved fully dense (99% of TD) nanoceramics with the application of hybrid radiant and microwave sintering. However, the second-step grain growth was not entirely suppressed in both radiant and microwave sintering, but the rapid growth observed in conventionally sintered samples was controlled. Application of TSS also enhances the hardness (12–14 GPa), fracture toughness 5–9  $\text{MPa m}^{1/2}$  and bending strength (900–1100) MPa [61, 62].

Despite the fulfilment of zirconia in a wide variety of application, it suffers from low-temperature degradation in the humid atmosphere around 65–500°C, with hinder biomedical application. Recently Sutharsini et al. [62] sintered fully dense (99% of TD) 3Y-TZP via TSS with average grain size 290 nm. The sintered ceramics exhibited better hydrothermal ageing resistance against the conventionally sintered 3Y-TZP ceramics.

#### 2.2.1.2. Sintering of 8YSZ

8YSZ ceramic is a promising candidate as a solid electrolyte for fuel cell application. Maca et al. [5] reported that efficiency of TSS depends on the crystal structure of the ceramics. The authors claimed that cubic structure has higher efficiency in controlling growth than hexagonal and tetragonal structures. Hence, TSS on 8YSZ controls the grain growth compared to 3Y-TZP due to its cubic crystal structure. TSS has been widely applied to 8YSZ to improve mechanical, electrical as well as the gas permeance via controlling the grain growth [3, 9, 24, 32–34]. It enhance the hardness (~13 GPa) [9, 32, 63], fracture toughness (3 MPam<sup>1/2</sup>) [9, 32, 63] and ionic conductivity (0.3 Scm<sup>-1</sup>) [9]. In addition to the above property, it is necessary to control grain growth to achieve optimum ratio of grain size to electrolyte layer thickness ( $0.1 < z < 0.3$ ) to control gas permeance value for SOFC [64]. TSS effectively controls gas permeance value [26].

Hesabi et al. [9] reported that the TSS is efficient in obtaining fine grain 8YSZ when compared to conventional and microwave sintering with nearly full density. The grain size and conductivity of conventionally sintered sample at 1500°C with a heating rate of 5°C/min, microwave-sintered samples at 1500°C with a heating rate of 50°C/min and TSS with the first-step sintering temperature of 1250°C with no holding time and the second-step sintering temperature of 1050°C with 20 h holding time were compared. The grain sizes were reported as 2.15 µm, 0.9 µm and 295 nm, and the conductivity at 1000°C were 255.4, 322.6 and 398.6 mS/cm for conventional, microwave and two-step sintered samples, respectively.

#### 2.2.2. Sintering of aluminium-based ceramics

Alumina-based ceramics are widely used for optical and biomedical applications. It is also used as filler for plastic and cutting inserts. However, the brittle nature of alumina limits the application. Ultrafine grain microstructure is crucial to enhance the mechanical properties such as hardness, wear resistance and strength. TSS successfully applied doped and pure alumina [5, 24, 25, 35–41]. Bodišová et al. [36] and others [5, 25, 35, 37, 39] successfully sintered fully dense alumina (98%) with controlled grain growth (grain growth below five times than that of powder size). Furthermore, the sample sintered with TSS exhibits excellent hardness (18 GPa) and fracture toughness (4 MPam<sup>1/2</sup>) [35].

It is also reported that the room temperature cooling between the first and second steps of sintering also affects the grain growth suppression of corundum abrasives. The TSS with 1250°C first-step temperature and 1350°C with a second-step temperature of 1150°C for 5 h yielded fine-grained corundum abrasives with grain sizes of 65 and 80 nm, respectively. The samples sintered at the same sintering profiles with a room temperature cooling yielded grain sizes of 400 and 560 nm, respectively. The conventional sintering at 1300°C for 2 h resulted to a final grain

size of 800 nm [43]. In addition, the two-step sintered corundum abrasive exhibited excellent hardness (22 GPa), fracture toughness (3 MPam<sup>1/2</sup>) and wear resistance ( $<2 \times 10^{-7}$  mm<sup>3</sup>/Nm) [43].

### 2.2.3. Sintering of YAG ( $Y_3Al_5O_{12}$ )

YAG is a familiar ceramic material for luminescent materials. Presently, single crystalline YAG is applied in lasers pumped by solid-state LEDs, scintillators, and infrared windows. Generally, YAG is sintered for high temperature and long holding time which leads to abnormal grain growth. TSS is an efficient and economic method, which control the abnormal grain growth and improved the transmittance of YAG [44, 45]. YAG sintered with the first-step sintering temperature at 1800°C and the second-step sintering temperature 1550–1600°C revealed more than 40% transmission [44, 45]. Furthermore, neodymium-doped YAG (Nd:YAG) sintered via TSS exhibited excellent transmittance (85%) [65].

### 2.2.4. Sintering of hydroxyapatite (HA)

Hydroxyapatite is a bioceramic that is used as tissue implants due to its excellent biocompatibility. However, low toughness hinders application of artificial bone and teeth implants. Furthermore, the major drawback of HA is that it decomposed into secondary phases ( $\alpha$ - or  $\beta$ -tricalcium phosphate). In order to avoid such decomposition, TSS has been applied to HA [14, 47–51, 66, 67]. Feng et al. [14] and others [14, 49, 50, 66, 67] successfully sintered monophase HA without decomposition. Furthermore, TSS improved mechanical properties. Mazaheri et al. [50] achieved highest hardness (7.8 GPa) and fracture toughness (1.9 MPam<sup>1/2</sup>) via TSS.

### 2.2.5. Sintering of Ni-Cu-Zn ferrite

Ni-Cu-Zn ferrite ceramics received special attention due to its low cost, excellent heat and corrosion resistance, high magnetic permeability and low magnetic loss. It is used in many electronic devices such as multilayer capacitor, sensors, antennas and broadband transformers. The electromagnetic properties of Ni-Cu-Zn ferrite are controlled by its microstructure and densification. Wang et al. [17] and Su et al. [68, 69] successfully sintered Ni-Cu-Zn ferrite by using TSS. Wang et al. [17] proposed kinetic window for successful TSS. Ni-Cu-Zn ferrite sintered by using TSS exhibited excellent magnetic properties [68, 69]. Magneto-dielectric materials with matched permeability and permittivity are promising candidates as loading materials to reduce the physical dimensions of low-frequency antennas. Ni-Cu-Zn ferrite sintered via TSS revealed almost equal permeability and permittivity of around 11.8. And the magnetic and dielectric loss tangents were lower than 0.015 in a frequency range from 10 to 100 MHz. These properties make the material useful to the design of miniaturized antennas [69].

### 2.2.6. Sintering of Si-based ceramics

Silicon carbide is widely used for abrasives and refractories due to its high strength, hardness and excellent thermal shock resistance. In conventional single-step sintering, abnormal grain growth is progressed due to its high sintering temperature. Generally, the grain

growth during the sintering in the presence of liquid phase is much more significant than that of solid-state sintering. Therefore, it is practically impossible to obtain nanostructured ceramics by conventional single-step liquid-phase sintering. TSS was successfully applied in liquid-phase-sintered SiC ceramics, and a fully dense nanostructured SiC ceramic with a grain size of ~40 nm has been obtained [58, 59] in argon atmosphere. Magnani et al. [60, 70] also successfully sintered doped SiC via TSS with enhanced mechanical properties. The sintered samples exhibited excellent hardness (24 GPa), fracture toughness (3 MPam<sup>1/2</sup>), Young modulus (400 GPa) and flexural strength (500 MPa).

Similar to SiC, silicon nitride, also non-oxide ceramics, exhibits high hardness strength and thermal shock resistance. It is widely applied to automotive engine wear parts due to its outstanding mechanical properties and wear resistance. Bimodal microstructure of silicon nitride was successfully sintered by using TSS without using  $\beta$ -Si<sub>3</sub>N<sub>4</sub> seed crystal [10, 71]. Bimodal microstructure enhances strength and toughness of the ceramic via crack bridging toughness mechanism [72]. Barium aluminosilicate-reinforced silicon nitride sintered via TSS also exhibited higher flexural strength (565 MPa) and fracture toughness (7 MPam<sup>1/2</sup>). The obtained composite exhibits excellent mechanical properties compared to unreinforced barium aluminosilicate matrix [10].

The forsterite (Mg<sub>2</sub>SiO<sub>4</sub>) ceramic is a new bioceramic with good biocompatibility. Forsterite sintered with the first-step sintering temperature 1300°C and the second-step sintering temperature at 750°C for 15 h revealed high density (98.5%) with grain size 300 nm. Furthermore it exhibited fracture toughness of 3.61 MPam<sup>1/2</sup>. Compared with hydroxyapatite ceramics, forsterite shows a significant improvement in the fracture toughness. Authors suggested that the two-step sintering method can be used to fabricate improved forsterite dense ceramics with desired bioactivity and mechanical properties that might be suitable for hard tissue repair and biomedical applications [51].

### 2.2.7. Sintering of alkaline niobate-based lead-free piezoelectric ceramics

Environmental friendly lead-free alkaline-based niobate ceramics exhibited excellent piezoelectric properties compared to Pb(Zr,Ti)O<sub>3</sub> ceramics. Alkaline-based niobate (KNN) ceramics are successfully sintered by using TSS, and they exhibited excellent dielectric [12, 55, 73], ferroelectric [12, 55, 56, 73] and piezoelectric properties [12, 21, 55, 56]. Furthermore (K<sub>0.4425</sub>Na<sub>0.52</sub>Li<sub>0.0375</sub>)(Nb<sub>0.8925</sub>Sb<sub>0.07</sub>Ta<sub>0.0375</sub>)O<sub>3</sub> exhibited excellent temperature stability over a wide range of temperature, which is attractive for piezoelectric applications [12].

### 2.2.8. Sintering of zinc oxide

Zinc oxide has been widely applied to electronic and optical devices. Furthermore, alumina-doped ZnO is used as an alternative to indium-doped tin oxide (ITO) as a transparent conductive electrode in photovoltaic devices and displays. Electrical and optical properties of ZnO are mainly influenced by grain size. Grain growth of ZnO was successfully controlled using TSS [16, 20, 22, 74–78]. Zhang et al. [20] and others [16] successfully sintered fully dense

ZnO without grain growth at the final stage of sintering. Furthermore Zhang et al. proposed kinetic window for successful TSS profile. Mazaheri et al. [22] confirmed the triple-point drag mechanism for controlled grain growth at the second-step sintering proposed by Chen and Wang [15] by using TEM image of two-step sintered ZnO compacts. ZnO sintered via TSS exhibited excellent I–V characteristics [16, 74, 76]. ZnO varistors sintered via TSS exhibited higher breakdown field of 6–8 kVmm<sup>-1</sup> and nonlinear coefficient of over 270 due to fine grain size and high concentration of ZnO–ZnO grain contacts [16].

### 2.2.9. Sintering of BaTiO<sub>3</sub>

Barium titanate (BaTiO<sub>3</sub>) is a polycrystalline piezoelectric ceramic. It is widely used to piezoelectric transducers, sensors and actuators. Many TSS studies have been conducted on BaTiO<sub>3</sub> [17, 79–90]. Barium titanate ceramic is widely applied to multilayered ceramic capacitors (MLCC), transducers and pyroelectric detectors due to its dielectric, ferroelectric and piezoelectric properties. Wang et al. [17, 83] successfully sintered fully dense nanostructured ceramic and proposed kinetic window for successful TSS. TSS not only improved the densification and grain growth but also enhanced dielectric and piezoelectric properties [79, 81, 82, 85–88, 91, 92]. TSS samples exhibited excellent piezoelectric constant 519 pN/C and relative permittivity of 6079 [82, 92]. Tian et al. [86] reported that TSS revealed excellent dielectric constant of 2400 at room temperature, low dielectric loss (<1%) and high insulation resistivity of 10<sup>12</sup> Ωcm, which could be beneficial for multilayer capacitor application.

## 3. TSS with low first-step sintering temperature

In few TSS studies, samples were initially heated to lower temperatures and then to higher temperature as shown in **Figure 1(b)**. Here the first step is normally a pre-coarsening step that is performed for several purposes including removal of volatile fraction and smoothing the pore channels. This method was successful to prepare fully dense nano-sized pure ZrO<sub>2</sub>, fully dense (>98%) alumina [38, 40] and alumina-doped zirconia (7.5Al<sub>2</sub>O<sub>3</sub>–92.5ZrO<sub>2</sub>) (vol.%) [8].

Sintering of pure zirconia has major drawback due to its reversible tetragonal-to-monoclinic phase transformation associated with shape deformation. Tartaj and Tartaj [93] applied TSS for pure zirconia below the phase transition temperature (<1150°C). In the first step, the compact allowed to achieve 96% of the density at 950°C for 10 h, and then the second-stage sintering temperature increased to 1050°C and achieved fully dense crack-free pure zirconia with grain size less than 200 nm.

Fully dense (99%) alumina-doped zirconia (7.5Al<sub>2</sub>O<sub>3</sub>–92.5ZrO<sub>2</sub>) (vol.%) is also successfully sintered by using microwave TSS by using lower first-step sintering temperature. Furthermore, microwave-assisted TSS revealed higher density (99%), hardness (13 GPa), fracture toughness (12 MPam<sup>1/2</sup>) and bending strength (750 MPa) than the conventional single-step sintering. Alumina-toughened zirconia is widely applied to dental implant due to its excellent biocompatibility and hardness [8].

Al<sub>2</sub>O<sub>3</sub> ceramics are also known as a better translucent with gas-impermeable properties which is suitable for high-pressure lamp envelopes. The high optical transmittance requires special efforts to eliminate any light scattering centres such as residual pores, grain boundaries, secondary phases and rough surfaces in the material. MgO-doped alumina ceramic sintered by TSS with lower first-step sintering exhibited improved the transmittance compared to conventionally sintered sample [40].

#### 4. Conclusion

Despite long holding times, TSS with higher first-step sintering temperature is convenient to achieve fully dense and fine-grained microstructured ceramics with improved properties. The TSS is successfully applied to a range of ceramic materials, and their application is broadened. TSS also helped the emergence of sintering as a fabrication technique. Tailoring the TSS conditions and theoretical studies on TSS mechanisms will make TSS a cost-effective method to fabricate advanced ceramics. TSS can also be studied by using different sintering methods and sintering environments in the first and second steps of sintering.

#### Author details

Ubenthiran Sutharsini<sup>1\*</sup>, Murugathas Thanihaichelvan<sup>1</sup> and Ramesh Singh<sup>2</sup>

\*Address all correspondence to: [ubsutharsini@gmail.com](mailto:ubsutharsini@gmail.com)

<sup>1</sup> Department of Physics, Faculty of Science, University of Jaffna, Jaffna, Sri Lanka

<sup>2</sup> Department of Mechanical Engineering, Faculty of Engineering, University of Malaya, Kuala Lumpur, Malaysia

#### References

- [1] Suárez G, Sakka Y, Suzuki TS, Uchikoshi T, Zhu X, Aglietti EF. Effect of starting powders on the sintering of nanostructured ZrO<sub>2</sub> ceramics by colloidal processing. *Science and Technology of Advanced Materials*. 2009;**10**:025004(1-8). DOI: 10.1088/1468-6996/10/2/025004/meta
- [2] Kim HD, Han BD, Park DS, Lee BT, Becher PF. Novel two-step sintering process to obtain a bimodal microstructure in silicon nitride. *Journal of the American Ceramic Society*. 2002;**85**:245-252. DOI: 10.1111/j.1151-2916.2002.tb00073.x
- [3] Schwarz S, Guillon O. Two step sintering of cubic yttria stabilized zirconia using Field Assisted Sintering Technique/Spark Plasma Sintering. *Journal of the European Ceramic Society*. 2013;**33**:637-641. DOI: 10.1016/j.jeurceramsoc.2012.10.002

- [4] Xiong Y, Hu J, Shen Z. Dynamic pore coalescence in nanoceramic consolidated by two-step sintering procedure. *Journal of the European Ceramic Society*. 2013;**33**:2087-2092. DOI: 10.1016/j.jeurceramsoc.2013.03.015
- [5] Maca K, Pouchly V, Zalud P. Two-step sintering of oxide ceramics with various crystal structures. *Journal of the European Ceramic Society*. 2010;**30**:583-589. DOI: 10.1016/j.jeurceramsoc.2009.06.008
- [6] Ubenthiran S, Ramesh S, Tan CY, Teng WD. Oxygen vacancy comparisons for 3Y-TZP sintered in air and argon gas atmosphere. *Applied Mechanics and Materials*. 2013;**372**:173-176. DOI: 10.4028/www.scientific.net/AMM.372.173
- [7] Sutharsini U, Ramesh S, Purbolaksono J, Tan CY, Teng WD, Amiriyan M. Low-temperature degradation and defect relationship in yttria-tetragonal zirconia polycrystal ceramic. *Materials Research Innovations*. 2014;**18**:S6-131-S136-134. DOI: 10.1179/1432891714Z.000000000943
- [8] Ai Y, Xie X, He W, Liang B, Fan Y. Microstructure and properties of  $\text{Al}_2\text{O}_3$  (n)/ $\text{ZrO}_2$  dental ceramics prepared by two-step microwave sintering. *Materials & Design*. 2015;**65**:1021-1027. DOI: 10.1016/j.matdes.2014.10.054
- [9] Hesabi ZR, Mazaheri M, Ebadzadeh T. Enhanced electrical conductivity of ultrafine-grained  $8\text{Y}_2\text{O}_3$  stabilized  $\text{ZrO}_2$  produced by two-step sintering technique. *Journal of Alloys and Compounds*. 2010;**494**:362-365. DOI: 10.1016/j.jallcom.2010.01.046
- [10] Ye F, Liu L, Zhang J, Iwasa M, Su CL. Synthesis of silicon nitride-barium aluminosilicate self-reinforced ceramic composite by a two-step pressureless sintering. *Composites Science and Technology*. 2005;**65**:2233-2239. DOI: 10.1016/j.compscitech.2005.04.015
- [11] Mazaheri M, Zahedi AM, Haghghatzadeh M, Sadrnezhaad SK. Sintering of titania nanoceramic: Densification and grain growth. *Ceramics International*. 2009;**35**:685-691. DOI: 10.1016/j.ceramint.2008.02.005
- [12] Pang X, Qiu J, Zhu K, Du J. (K, Na) $\text{NbO}_3$  based lead free piezoelectric ceramics manufactured by two step sintering. *Ceramics International*. 2012;**38**:2521-2527. DOI: 10.1016/j.ceramint.2011.11.022
- [13] Khosroshahi HR, Ikeda H, Yamada K, Saito N, Kaneko K, Hayashi K, Nakashima K. Effect of cation doping on mechanical properties of yttria prepared by an optimized two-step sintering process. *Journal of the American Ceramic Society*. 2012;**95**:3263-3269. DOI: 10.1111/j.1551-2916.2012.05379.x
- [14] Feng P, Niu M, Gao C, Peng S, Shuai C. A novel two-step sintering for nano-hydroxyapatite scaffolds for bone tissue engineering. *Scientific Reports*. 2014;**4**:5599. DOI: 10.1038/srep05599
- [15] Chen IW, Wang XH. Sintering dense nanocrystalline ceramics without final-stage grain growth. *Nature*. 2000;**404**:168-171. DOI: 10.1038/35004548
- [16] Durán P, Tartaj J, Moure C. Fully dense, fine-grained, doped zinc oxide varistors with improved nonlinear properties by thermal processing optimization. *Journal of the American Ceramic Society*. 2003;**86**:1326-1329. DOI: 10.1111/j.1151-2916.2003.tb03470.x

- [17] Wang XH, Deng XY, Bai HL, Zhou H, Qu WG, Li LT, Chen IW. Two-step sintering of ceramics with constant grain-size, II: BaTiO<sub>3</sub> and Ni-Cu-Zn Ferrite. *Journal of the American Ceramic Society*. 2006;**89**:438-443. DOI: 10.1111/j.1551-2916.2005.00728.x
- [18] Ding J, Liu Y, Lu Y, Qian H, Gao H, Chen H, Ma C. Enhanced energy-storage properties of 0.89Bi<sub>0.5</sub>Na<sub>0.5</sub>TiO<sub>3-0.06</sub>BaTiO<sub>3-0.05</sub>K<sub>0.5</sub>Na<sub>0.5</sub>NbO<sub>3</sub> lead-free anti-ferroelectric ceramics by two-step sintering method. *Materials Letters*. 2014;**114**:107-110. DOI: 10.1016/j.matlet.2013.09.103
- [19] Wang XH, Chen PL, Chen IW. Two-step sintering of ceramics with constant grain-size, I. Y<sub>2</sub>O<sub>3</sub>. *Journal of the American Ceramic Society*. 2006;**89**:431-437. DOI: 10.1111/j.1551-2916.2005.00763
- [20] Zhang Y, Tan R, Yang Y, Zhang X, Wang W, Cui P, Song W. Two-step sintering of pristine and aluminum-doped zinc oxide ceramics. *International Journal of Applied Ceramic Technology*. 2012;**9**:960-967. DOI: 10.1111/j.1744-7402.2011.02702.x
- [21] Zou T, Wang X, Zhao W, Li L. Preparation and properties of fine-grain (1-x) BiScO<sub>3-x</sub>PbTiO<sub>3</sub> ceramics by two-step sintering. *Journal of the American Ceramic Society*. 2008;**91**:121-126. DOI: 10.1111/j.1551-2916.2007.01903.x
- [22] Mazaheri M, Zahedi AM, Sadrnezhad SK. Two-step sintering of nanocrystalline ZnO compacts: effect of temperature on densification and grain growth. *Journal of the American Ceramic Society*. 2008;**91**:56-63. DOI: 10.1111/j.1551-2916.2007.02029.x
- [23] He R, Zhang R, Pei Y, Fang D. Two-step hot pressing of bimodal micron/nano-ZrB<sub>2</sub> ceramic with improved mechanical properties and thermal shock resistance. *International Journal of Refractory Metals and Hard Materials*. 2014;**46**:65-70. DOI: 10.1016/j.ijrmhm.2014.05.016
- [24] Pouchly V, Maca K, Shen Z. Two-stage master sintering curve applied to two-step sintering of oxide ceramics. *Journal of the European Ceramic Society*. 2013;**33**:2275-2283. DOI: 10.1016/j.jeurceramsoc.2013.01.020
- [25] Maca K, Pouchly V, Shen Z. Two-step sintering and spark plasma sintering of Al<sub>2</sub>O<sub>3</sub>, ZrO<sub>2</sub> and SrTiO<sub>3</sub> ceramics. *Integrated Ferroelectrics*. 2008;**99**:114-124. DOI: 10.1080/10584580802107841
- [26] Wright GJ, Yeomans JA. Constrained sintering of yttria-stabilized zirconia electrolytes: The influence of two-step sintering profiles on microstructure and gas permeance. *International Journal of Applied Ceramic Technology*. 2008;**5**:589-596. DOI: 10.1111/j.1744-7402.2008.02263.x
- [27] Wright GJ, Yeomans JA. Three-step sintering of constrained yttria stabilised zirconia layers and its effect on microstructure and gas permeance. *Journal of the European Ceramic Society*. 2009;**29**:1933-1938. DOI: 10.1016/j.jeurceramsoc.2008.12.013
- [28] Mazaheri M, Simchi A, Golestani-Fard F. Densification and grain growth of nanocrystalline 3Y-TZP during two-step sintering. *Journal of the European Ceramic Society*. 2008;**28**:2933-2939. DOI: 10.1016/j.jeurceramsoc.2008.04.030

- [29] Lourenço MA, Cunto GG, Figueiredo FM, Frade JR. Model of two-step sintering conditions for yttria-substituted zirconia powders. *Materials Chemistry and Physics*. 2011;**126**:262-271. DOI: 10.1016/j.matchemphys.2010.11.028
- [30] Suarez G, Sakka Y, Suzuki TS, Uchikoshi T, Aglietti EF. Effect of bead-milling treatment on the dispersion of tetragonal zirconia nanopowder and improvements of two-step sintering. *Journal of the Ceramic Society of Japan*. 2009;**117**:470-474. DOI: 10.2109/jcersj2.117.470
- [31] Binner J, Annapoorani K, Paul A, Santacruz I, Vaidhyanathan B. Dense nanostructured zirconia by two stage conventional/hybrid microwave sintering. *Journal of the European Ceramic Society*. 2008;**28**:973-977. DOI: 10.1016/j.jeurceramsoc.2007.09.002
- [32] Mazaheri M, Valefi M, Hesabi ZR, Sadrnezhaad S. Two-step sintering of nanocrystalline  $8Y_2O_3$  stabilized  $ZrO_2$  synthesized by glycine nitrate process. *Ceramics International*. 2009;**35**:13-20. DOI: 10.1016/j.jeurceramsoc.2007.09.002
- [33] Rajeswari K, Hareesh U, Subasri R, Chakravarty D, Johnson R. Comparative evaluation of spark plasma (SPS), microwave (MWS), two stage sintering (TSS) and conventional sintering (CRH) on the densification and microstructural evolution of fully stabilized zirconia ceramics. *Science of Sintering*. 2010;**42**:259-267. DOI: 10.2298/SOS1003259R
- [34] Laberty-Robert C, Ansart F, Deloget C, Gaudon M, Rousset A. Dense yttria stabilized zirconia: sintering and microstructure. *Ceramics International*. 2003;**29**:151-158. DOI: 10.1016/S0272-8842(02)00099-8
- [35] Razavi Hesabi Z, Haghghatzadeh M, Mazaheri M, Galusek D, Sadrnezhaad S. Suppression of grain growth in sub-micrometer alumina via two-step sintering method. *Journal of the European Ceramic Society*. 2009;**29**:1371-1377. DOI: 10.1016/j.jeurceramsoc.2008.08.027
- [36] Bodišová K, Šajgalík P, Galusek D, Švančárek P. Two-stage sintering of alumina with submicrometer grain size. *Journal of the American Ceramic Society*. 2007;**90**:330-332. DOI: 10.1111/j.1551-2916.2006.01408.x
- [37] Galusek D, Ghillányová K, Sedláček J, Kozánková J, Šajgalík P. The influence of additives on microstructure of sub-micron alumina ceramics prepared by two-stage sintering. *Journal of the European Ceramic Society*. 2012;**32**:1965-1970. DOI: 10.1016/j.jeurceramsoc.2011.11.038
- [38] Lin FJT, de Jonghe LC, Rahaman MN. Microstructure refinement of sintered alumina by a two-step sintering technique. *Journal of the American Ceramic Society*. 1997;**80**:2269-2277. DOI: 10.1111/j.1151-2916.1997.tb03117.x
- [39] Michálková M, Ghillányová K, Galusek D. Standard and two-stage sintering of a submicrometer alumina powder. In: RK Bordia, EA Olevsky. *Advances in Sintering Science and Technology*, John Wiley & Sons, Inc.; Hoboken, NJ, USA; 2010. 421 p. DOI: 10.1002/9780470599730.ch40

- [40] Kim DS, Lee JH, Sung RJ, Kim SW, Kim HS, Park JS. Improvement of translucency in  $\text{Al}_2\text{O}_3$  ceramics by two-step sintering technique. *Journal of the European Ceramic Society*. 2007;**27**:3629-3632. DOI: 10.1016/j.jeurceramsoc.2007.02.002
- [41] Wang CJ, Huang CY, Wu YC. Two-step sintering of fine alumina–zirconia ceramics. *Ceramics International*. 2009;**35**:1467-1472. DOI: 10.1016/j.ceramint.2008.08.001
- [42] Sairam K, Sonber J, Murthy TC, Sahu A, Bedse R, Chakravartty J. Pressureless sintering of chromium diboride using spark plasma sintering facility. *International Journal of Refractory Metals and Hard Materials*. 2016;**58**:165-171. DOI: 10.1016/j.ijrmhm.2016.05.002
- [43] Li Z, Li Z, Zhang A, Zhu Y. Synthesis and two-step sintering behavior of sol–gel derived nanocrystalline corundum abrasives. *Journal of the European Ceramic Society*. 2009;**29**:1337-1345. DOI: 10.1016/j.jeurceramsoc.2008.09.004
- [44] Chen ZH, Li JT, Xu JJ, Hu ZG. Fabrication of YAG transparent ceramics by two-step sintering. *Ceramics International*. 2008;**34**:1709-1712. DOI: 10.1016/j.ceramint.2007.05.015
- [45] Li X, Zheng B, Odoom-Wubah T, Huang J. Co-precipitation synthesis and two-step sintering of YAG powders for transparent ceramics. *Ceramics International*. 2013;**39**:7983-7988. DOI: 10.1016/j.ceramint.2013.03.064
- [46] Liu J, Lv X, Li J, Jiang L. Pressureless sintered magnesium aluminate spinel with enhanced mechanical properties obtained by the two-step sintering method. *Journal of Alloys and Compounds*. 2016;**680**:133-138. DOI: 10.1016/j.jallcom.2016.04.192
- [47] Lukić M, Stojanović Z, Škapin SD, Maček-Kržmanc M, Mitrić M, Marković S, Uskoković D. Dense fine-grained biphasic calcium phosphate (BCP) bioceramics designed by two-step sintering. *Journal of the European Ceramic Society*. 2011;**31**:19-27. DOI: 10.1016/j.jeurceramsoc.2010.09.006
- [48] Panyata S, Eitssayeam S, Rujijanagul G, Tunkasiri T, Pengpat K. Property development of hydroxyapatite ceramics by two-step sintering. In: *Advanced Materials Research*, Trans Tech Publ; Zurich, Switzerland; 2012, p. 190-193. DOI: 10.4028/www.scientific.net/AMR.506.190
- [49] Lin K, Chen L, Chang J. Fabrication of dense hydroxyapatite nanobioceramics with enhanced mechanical properties via two-step sintering process. *International Journal of Applied Ceramic Technology*. 2012;**9**:479-485. DOI: 10.1111/j.1744-7402.2011.02654.x
- [50] Mazaheri M, Haghighatzadeh M, Zahedi AM, Sarnezhaad SK. Effect of a novel sintering process on mechanical properties of hydroxyapatite ceramics. *Journal of Alloys and Compounds*. 2009;**471**:180-184. DOI: 10.1016/j.jallcom.2008.03.066
- [51] Fathi MH, Kharaziha M. Two-step sintering of dense, nanostructural forsterite. *Materials Letters*. 2009;**63**:1455-1458. DOI: 10.1016/j.matlet.2009.03.040

- [52] Mazaheri M, Razavi Hesabi Z, Sadrnezhad SK. Two-step sintering of titania nanoceramics assisted by anatase-to-rutile phase transformation. *Scripta Materialia*. 2008;**59**: 139-142. DOI: 10.1016/j.scriptamat.2008.02.041
- [53] Li D, Chen SO, Shao WQ, Wang DC, Li YH, Long YZ, Liu ZW, Ringer SP. Preparation of dense nanostructured titania ceramic using two step sintering. *Materials Technology*. 2010;**25**:42-44. DOI: 10.1179/175355509X12608871787997
- [54] Li BR, Liu DY, Liu JJ, Hou SX, Yang ZW. Two-step sintering assisted consolidation of bulk titania nano-ceramics by spark plasma sintering. *Ceramics International*. 2012;**38**:3693-3699. DOI: 10.1016/j.ceramint.2012.01.011
- [55] Fang J, Wang X, Tian Z, Zhong C, Li L, Zuo R. Two-step sintering: An approach to broaden the sintering temperature range of alkaline niobate-based lead-free piezoceramics. *Journal of the American Ceramic Society*. 2010;**93**:3552-3555. DOI: 10.1111/j.1551-2916.2010.04085.x
- [56] Hao J, Bai W, Shen B, Zhai J. Improved piezoelectric properties of  $(K_xNa_{1-x})_{0.94}Li_{0.06}NbO_3$  lead-free ceramics fabricated by combining two-step sintering. *Journal of Alloys and Compounds*. 2012;**534**:13-19. DOI: 10.1016/j.jallcom.2012.04.033
- [57] Lartcumfu N, Kruea-In C, Tawichai N, Rujijanagul G. Fabrication of sodium potassium niobate ceramics by two step sintering assisted molten salts synthesis. *Ferroelectrics*. 2013;**456**:14-20. DOI: 10.1080/00150193.2013.846171
- [58] Lee YI, Kim YW, Mitomo M. Effect of processing on densification of nanostructured SiC ceramics fabricated by two-step sintering. *Journal of Material Science*. 2004;**39**:3801-3803. DOI: 10.1023/B:JMSC.0000030743.62306.70
- [59] Lee YI, Kim YW, Mitomo M, Kim DY. Fabrication of dense nanostructured silicon carbide ceramics through two-step sintering. *Journal of the American Ceramic Society*. 2003;**86**:1803-1805. DOI: 10.1111/j.1151-2916.2003.tb03560.x
- [60] Magnani G, Sico G, Brentari A. Two-Step Pressureless Sintering of Silicon Carbide-Based Materials; In: Pietro Vincenzini. *Advances in Science and Technology*, Trans Tech Publ; Zurich, Switzerland; 2014, p. 70-75. DOI:10.4028/www.scientific.net/AST.89.70
- [61] Chao M, Ning L, Zhikai W, Jing T, Jiazhen Y. Influence on microstructure of dental zirconia ceramics prepared by two-step sintering. *West China Journal of Stomatology*. 2013;**31**, 496-499. DOI: 10.7518/hxkq.2013.05.013
- [62] Sutharsini U, Ramesh S, Wong YH, Misran H, Yusuf F, Tan CY, Purbolaksono J, Teng WD. Effect of sintering holding time on low-temperature degradation of yttria stabilised zirconia ceramics. *Materials Research Innovations*. 2014;**18**:S6-408-S406-411. DOI: 10.1179/1432891714Z.000000000988
- [63] Mazaheri M, Zahedi A, Hejazi M. Processing of nanocrystalline 8 mol% yttria-stabilized zirconia by conventional, microwave-assisted and two-step sintering. *Materials Science and Engineering*. 2008;**492**:261-267. DOI: 10.1016/j.msea.2008.03.023

- [64] Wright GJ, Yeomans JA. The influence of screen-printing parameters on the microstructure and gas permeance of a zirconia electrolyte. *Journal of the European Ceramic Society*. 2008;**28**:779-785. DOI: 10.1016/j.jeurceramsoc.2007.09.027
- [65] Li J, Chen Q, Feng G, Wu W, Xiao D, Zhu J. Optical properties of the polycrystalline transparent Nd: YAG ceramics prepared by two-step sintering. *Ceramics International*. 2012;**38**:S649-S652. DOI: 10.1016/j.ceramint.2011.05.127
- [66] Chu KT, Ou SF, Chen SY, Chiou SY, Chou HH, Ou KL. Research of phase transformation induced biodegradable properties on hydroxyapatite and tricalcium phosphate based bioceramic. *Ceramics International*. 2013;**39**:1455-1462. DOI: 10.1016/j.ceramint.2012.07.089
- [67] Veljovic D, Palcevskis E, Zalite I, Petrovic R, Janackovic D. Two-step microwave sintering – A promising technique for the processing of nanostructured bioceramics. *Materials Letters*. 2013;**93**:251-253. DOI: 10.1016/j.matlet.2012.11.095
- [68] Su H, Tang X, Zhang H, Zhong Z, Shen J. Sintering dense Ni-Zn ferrite by two-step sintering process. *Journal of Applied Physics*. 2011;**109**:07A501. DOI: 10.1063/1.3535418
- [69] Su H, Tang X, Zhang H, Jing Y, Bai F, Zhong Z. Low-loss Ni-Cu-Zn ferrite with matching permeability and permittivity by two-step sintering process. *Journal of Applied Physics*. 2013;**113**:17B301. DOI: 10.1063/1.4793508
- [70] Magnani G, Brentari A, Buresi E, Raiteri G. Pressureless sintered silicon carbide with enhanced mechanical properties obtained by the two-step sintering method. *Ceramics International*. 2014;**40**:1759-1763. DOI: 10.1016/j.ceramint.2013.07.075
- [71] Kim HD, Park YJ, Han BD, Park MW, Bae WT, Kim YW, Lin HT, Becher PF. Fabrication of dense bulk nano-Si<sub>3</sub>N<sub>4</sub> ceramics without secondary crystalline phase. *Scripta materialia*. 2006;**54**:615-619. DOI: 10.1016/j.scriptamat.2005.10.032
- [72] Becher PF. Microstructural design of toughened ceramics. *Journal of the American Ceramic Society*. 1991;**74**:255-269. DOI: 10.1111/j.1151-2916.1991.tb06872.x
- [73] Kato K, Kakimoto K, Hatano K, Kobayashi K, Doshida Y. Lead-free Li-modified (Na, K)NbO<sub>3</sub> piezoelectric ceramics fabricated by two-step sintering method. *Journal of the Ceramic Society of Japan*. 2014;**122**:460-463. DOI: 10.2109/jcersj2.122.460
- [74] Pillai SC, Kelly JM, McCormack DE, Ramesh R. Effect of step sintering on breakdown voltage of varistors prepared from nanomaterials by sol gel route. *Advances in Applied Ceramics*. 2006;**105**:158-160. DOI: 10.1179/174367606X110189
- [75] Anas S, Mangalaraja R, Poothayal M, Shukla SK, Ananthakumar S. Direct synthesis of varistor-grade doped nanocrystalline ZnO and its densification through a step-sintering technique. *Acta Materialia*. 2007;**55**:5792-5801. DOI: 10.1016/j.actamat.2007.06.047
- [76] Shahraki M, Shojaee SA, Sani MA F, Nemati A, Safaee I. Two-step sintering of ZnO varistors. *Solid State Ionics*. 2011;**190**:99-105. DOI: 10.1016/j.ssi.2010.06.026

- [77] Chen B, Xia Z, Lu K. Understanding sintering characteristics of ZnO nanoparticles by FIB-SEM three-dimensional analysis. *Journal of the European Ceramic Society*. 2013;**33**:2499-2507. DOI: 10.1016/j.jeurceramsoc.2013.04.026
- [78] Wu MW. Two-step sintering of aluminum-doped zinc oxide sputtering target by using a submicrometer zinc oxide powder. *Ceramics International*. 2012;**38**:6229-6234. DOI: 10.1016/j.ceramint.2012.04.076
- [79] Takuya H, Kayo T, Jianyong L, Takeshi K, Hirofumi K, Takaaki T. Domain size effect on dielectric properties of barium titanate ceramics. *Japanese Journal of Applied Physics*. 2008;**47**:7607-7611. DOI: 10.1143/JJAP.47.7607/meta
- [80] Hoshina T, Kigoshi Y, Furuta T, Takeda H, Tsurumi T. Shrinkage behaviors and sintering mechanism of BaTiO<sub>3</sub> ceramics in two-step sintering. *Japanese Journal of Applied Physics*. 2011;**50**:09NC07-(1-4). DOI: 10.1143/JJAP.50.09NC07
- [81] Xu T, Wang CA. Effect of two-step sintering on micro-honeycomb BaTiO<sub>3</sub> ceramics prepared by freeze-casting process. *Journal of the European Ceramic Society*. 2016;**36**:2647-2652. DOI: 10.1016/j.jeurceramsoc.2016.03.032
- [82] Huan Y, Wang X, Fang J, Li L. Grain size effects on piezoelectric properties and domain structure of BaTiO<sub>3</sub> ceramics prepared by two-step sintering. *Journal of the American Ceramic Society*. 2013;**96**:3369-3371. DOI: 10.1111/jace.12601
- [83] Wang XH, Deng XY, Zhou H, Li LT, Chen IW. Bulk dense nanocrystalline BaTiO<sub>3</sub> ceramics prepared by novel pressureless two-step sintering method. *Journal of Electroceramics*. 2008;**21**:230-233. DOI: 10.1007/s10832-007-9143-1
- [84] Moon SM, Wang X, Cho NH. Nanostructural and physical features of BaTiO<sub>3</sub> ceramics prepared by two-step sintering. *Journal of the Ceramic Society of Japan*. 2009;**117**:729-731. DOI: 10.2109/jcersj2.117.729
- [85] Tian Z, Wang X, Lee S, Hur KH, Li L. Microstructure evolution and dielectric properties of ultrafine grained BaTiO<sub>3</sub>-based ceramics by two-step sintering. *Journal of the American Ceramic Society*. 2011;**94**:1119-1124. DOI: 10.1111/j.1551-2916.2010.04234.x
- [86] Tian Z, Wang X, Shu L, Wang T, Song TH, Gui Z, Li L. Preparation of nano BaTiO<sub>3</sub> based ceramics for multilayer ceramic capacitor application by chemical coating method. *Journal of the American Ceramic Society*. 2009;**92**:830-833. DOI: 10.1111/j.1551-2916.2009.02979.x
- [87] Karaki T, Yan K, Adachi M. Barium titanate piezoelectric ceramics manufactured by two-step sintering. *Japanese Journal of Applied Physics*. 2007;**46**:7035-7038. DOI: 10.1143/JJAP.46.7035
- [88] Polotai A, Breece K, Dickey E, Randall C, Ragulya A. A Novel approach to sintering nanocrystalline barium titanate ceramics. *Journal of the American Ceramic Society*. 2005;**88**:3008-3012. DOI: 10.1111/j.1551-2916.2005.00552.x
- [89] Kim HT, Han YH. Sintering of nanocrystalline BaTiO<sub>3</sub>. *Ceramics International*. 2004;**30**:1719-1723. DOI: 10.1016/j.ceramint.2003.12.141

- [90] Chaisan W, Yimnirun R, Ananta S. Two-stage sintering of barium titanate ceramic and resulting characteristics. *Ferroelectrics*. 2007;**346**:84-92. DOI: 10.1080/00150190601180380
- [91] Tomoaki K, Kang Y, Toshiyuki M, Masatoshi A. Lead-free piezoelectric ceramics with large dielectric and piezoelectric constants manufactured from BaTiO<sub>3</sub> nano-powder. *Japanese Journal of Applied Physics*. 2007;**46**:L97-L98. DOI: 10.1143/JJAP.46.L97/meta
- [92] Huan Y, Wang X, Fang J, Li L. Grain size effect on piezoelectric and ferroelectric properties of BaTiO<sub>3</sub> ceramics. *Journal of the European Ceramic Society*. 2014;**34**:1445-1448. DOI: 10.1016/j.jeurceramsoc.2013.11.030
- [93] Tartaj J, Tartaj P. Two-stage sintering of nanosize pure zirconia. *Journal of the American Ceramic Society*. 2009;**92**:S103-S106. DOI: 10.1111/j.1551-2916.2008.02723.x

IntechOpen

